# Variable Speed Control … for a Compact Humanoid Robot

Milton Ruas[†], Filipe M. Silva[†], Vítor M. Santos[*]
a23570@alunos.det.ua.pt, vsantos@mec.ua.pt, fsilva@det.ua.pt
[†]Department of Electronics and Telecommunications
[*]Department of Mechanical Engineering
University of Aveiro, 3810-193 Aveiro, Portugal

**Abstract**: no fim ☺

## 1.   Introduction

In recent years, the field of humanoid robotics has attracted the attention of a growing community, both from the industry and academia. It becomes increasingly evident the dichotomy in the styles used to design compact humanoid robots. On the one hand, several companies have unveiled walking robots with impressive designs and skills, as represented by Honda's ASIMO [1] and Sony's QRIO [2]. On the other hand, the continuous progress in robotics technology and the advances in computing hardware have promoted research on low-cost and easy-to-design humanoids, such as PINO [3], ESYS [4] and HanSaRam [4]. Here, the major challenge is to provide good performance of the control architecture and modularity at the system's level.

In this paper, we describe parts of the control system architecture for a small-size 22 degrees of freedom (DOF) humanoid robot. The research focuses on the distributed control architecture, with the emphasis being placed on how actuators are driven to achieve a desired performance. For the dimensions involved, off-the-shelf actuation technologies do not offer significant alternatives other than small servomotors, such as those from FUTABA, HITEC and similar. There are several general characteristics that have made them actuators of choice in a large number of other applications: small, compact and relatively inexpensive. In fact, the servomotor itself has built-in motor, gearbox, position feedback mechanism and controlling electronics.

However, this common method of driving a robotic joint can deeply influence the system's performance. First, it is well known that the control of the individual joints of the humanoid robot involves variation of the load inertia. Most certainly, such variations should be taken into account when trying to determine the proper control action; otherwise a decrease in performance will occur.

A second problem concerning the mentioned servomotors, is that they do not offer directly velocity control. Those servos can be controlled to move to any position just by using simple pulse width modulation (PWM). By design, servos drive to their commanded position fairly rapidly depending on the load (usually faster if the difference in position is larger).

A distributed set of microcontroller units is a key element to implement an adaptive scheme that compensates for the large changes in reflected inertia and providing variable velocity control.

Instead of changing the motor internals, as some other authors do, it was decided to improve its operation by software. That is achieved by a variable PWM throughout the full excursion of a joint. The algorithm is based on dynamic PWM tracking using the servo own potentiometer for feedback. In other words, the software tracks motor position with time and adjusts the PWM in order to accelerate or pause motor motion (the loop is closed back to the controller). Further, generating the control signals in each controller unit will reduce significantly the overhead on the controlling software.

## 2.   Project Overview and Framework

The main scope of the project beneath this paper has been the development of a humanoid platform to carry out research on control, navigation and perception, and also to offer opportunities for under and pos-graduate students to apply engineering methods and techniques in such ambitious and overwhelming endeavour. Purchasing a commercial platform carries prohibitive costs and it would reduce the involvement at the lowest levels of machine design, which was posed as a relevant pursuit for the desired engineering approach.

The ultimate goal of the project is to build a prototype capable of participating in the RoboCup humanoid league where a wide range of technologies need to be integrated and evaluated, giving added value for project-oriented education.
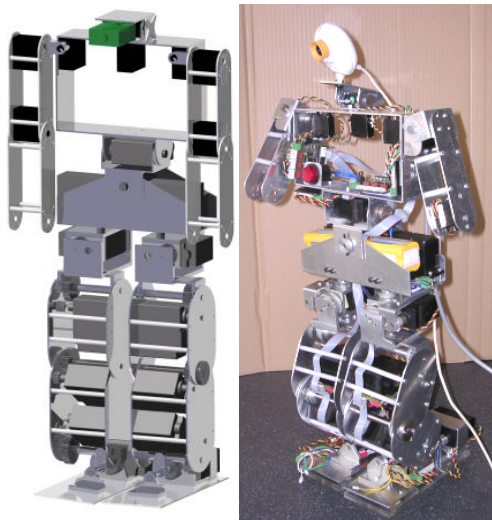
Fig. 1 - Model of the humanoid robot and current stage of implementation.

The most relevant achievements of this implementation include the distributed control architecture, based on a CAN bus, and the modularity at the system's level.

## 2.1 Mechanical Design

In what concerns the physical and functional requirements, the initial considerations were largely imposed by the rules of the ROBOCUP, namely, the robot dimensions, the mobility skills, the high level of autonomous operation and the selected tasks.

In order to ensure proper and versatile locomotion, the robot is doted with six DOFs per leg, namely one universal joint at the foot, a simple joint on the knee and a spherical joint on the hip. Connecting the legs to the upper structure of the abdomen was decided to be done with two DOFs mainly aiming at greater flexibility in balance control and account for the perturbations of the centre of mass (CoM). So far, arms have been only partially defined and the head accounts for two DOFs for the vision based perception.

A complete humanoid model and a view of the current stage of implementation are illustrated in Fig. 1. This is a small-size robot with 22 DOF's, about 64 cm height and 6 kg weight.

## 2.2 Actuators and Sensors

For the dimensions involved, off-the-shelf technologies of actuation do not offer significant alternatives other than small servomotors, such as those from FUTABA, HITEC and similar. HITEC servomotors were chosen in our application. Power to drive the motors is another central issue since servos require a high current, namely at start-up and when producing motion in some configurations. Two ion-lithium batteries were installed and the system counts with a 7.2 V/9600 mAh pack, with maximal sustained current specified at more than 19A.

Perception assumes a major role in an autonomous robot and, therefore, it must be reliable and abundant. For this platform the following perception is available: each joint position (reading servo own potentiometer), joint motor current (related to torque), force sensors on the feet to measure ground reaction forces, inclination of some links (using accelerometers), angular velocity of some links (using a gyro) and vision unit. Up to now, only vision has not yet been implemented on the system. The remainder sensors were addressed with different levels of accuracy, but all potentially usable with current hardware.

## 2.3 Distributed Control Approach

From the very beginning of the project, one major concern has been the development of a flexible control system to allow for short and possibly longer term developments. The key concept for the control architecture is the distributed approach, in which independent and self-contained tasks may allow a standalone operation. The platform was given a network of controllers connected by a CAN bus in a master-multi salve arrangement. Master and slave units are based on a PIC microcontroller. Fig. 2 shows a generic diagram of controlling units.

The master unit relays all slave units by dispatching medium and high level orders and by collecting sensorial data to be exchanged with the central unit. The central unit is currently an off-board computer but will be migrated to a local controller based on a PC104+ board with image processing capability.

Slaves can drive up to three servomotors, monitor their angular positions and electrical current consumption. The system joints have been grouped by vicinity criteria and are controlled by a dedicated board. Concerning additional sensors, each slave unit has the possibility of accepting a piggy-back board where additional circuit can lay to interface to other sensors (e.g., force-sensors, accelerometers and gyroscope).
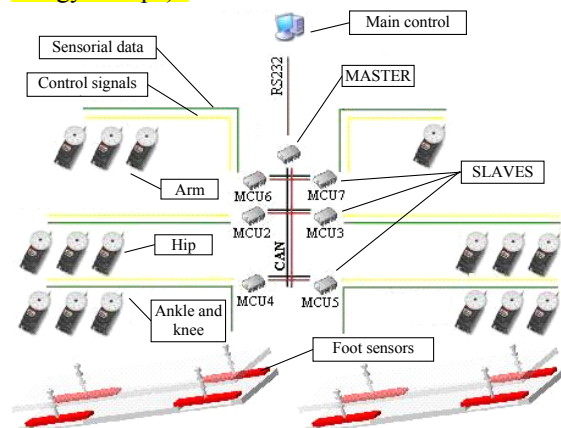


Fig. 2 - General architecture layout.

2

# 3. Servomotors and Their Control

## 3.1 Experimental Setup (section 2?)

## 3.2 Open-Loop Performance

- Load variation (step response)
- Set point control (table and graphs)
- Speed and current versus torque

We will now study the servo behaviour using only its internal controller to reach the set point requested. When we refer open loop state, we refer in the servo outside point of view, without introducing any external controller. We will start to study its behaviour to step inputs.
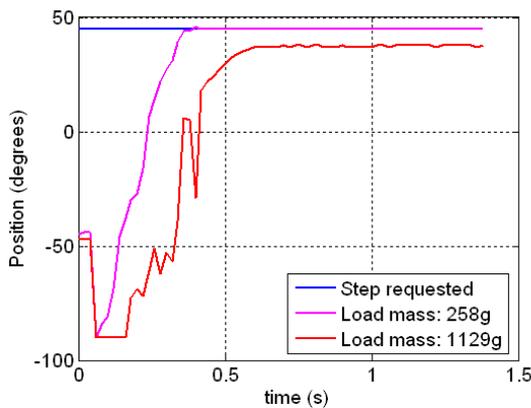


Fig. 3 - Step response for two loads from the position -45º to +45º.

Applying a step from -45º to +45º position for different loads, the first distinctive difference is the steady state errors. For the low mass the steady state error is practically negligible, but for the 1129g load we can measure a 8º error. Another characteristic observed is the unstable dynamic behavior with a jump to a position below of -45º and some oscillations during travel to the final set point. Nevertheless these conditions were not observed in reality showing a continuous and a fast motion to the final position without speed inversions nor oscillations. This tell us that when carrying out long trajectories at the maximum speed (characteristic in step responses) the potentiometer output tend to be unstable when increasing the load mass. This is related to the way this sensor is read: due to the not common ground in potentiometer measure on the servo side, its output signal only is consistent with the real servo position only when a very low current is being consumed. For high loads or fast movements the servo increases its current consumption and introduces an output impulse of amplitude above its standard voltage (correspondent to position) and synchronized periodically with the PWM signal, whose length is directly related to the current consumed (Fig.4).
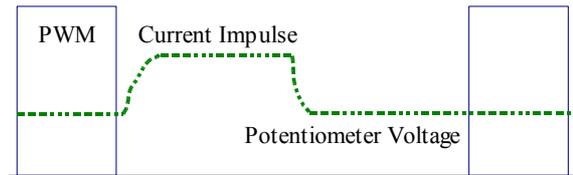


Fig. 4: Potentiometer voltage behavior in a PWM cycle.

To avoid measure interference, potentiometer times in each PWM period and only the minimal value is taken into account. Nevertheless for high loads the current impulse can cover all PWM period incapacitating position reading. That is what happens in Fig.3: the low peaks in the transient behavior correspond to high peaks in voltage caused by the current impulse interference. To avoid this kind of problems and guarantee the occurrence of finite current impulses so as to be able to measure the real potentiometer output, from now on we will only study the ramp response, a succession of steps of constant amplitude over time, relatively to the previous one, until final position is reached. This way the current consumption will only practically depend on the load torq exerted, because of the speed limitation introduced by the ramp input, and therefore the levels of current consumed will be lower. In addition, beyond the position control, velocity control is introduced by the definition of the ramp length.
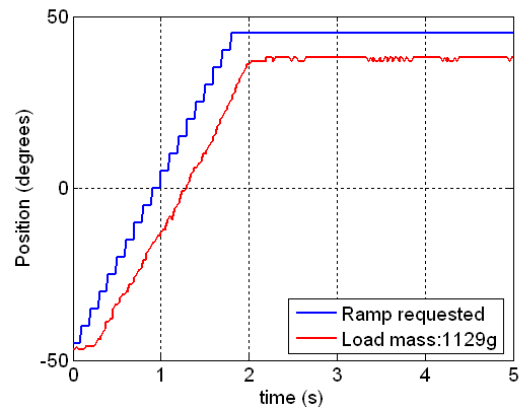


Fig. 5: Ramp response for the highest load.

Although the transient response has a very improved behavior, the steady state error continues present. Table 1 shows the results of an experiment realized to study this effect: a weight is requested to move to a set of defined positions, and for each one, we wait the completion of the movement and, afterwards, the potentiometer is sampled to obtain the real position where the servo is. Relating the positioning error with the tork exerted in the joint – $\cos(\theta)*m*g$, whith $\theta$ being the weight angular position, $m$ its mass and $g$ the gravity acceleration – we find a notorious relation between them: as higher is the torq, higher is the steady state error. This lead us to think that the servo internal controller does not possess an integrator module which would bring the

3

steady state error to zero, independently of the existing torq.

| Requested position | Effective position | Error | Torq exerted |
|---|---|---|---|
| -80 | -80 | 0 | 0.198 |
| -60 | -62 | 2 | 0.569 |
| -40 | -45 | 5 | 0.872 |
| -20 | -28 | 8 | 1.069 |
| 0 | -9 | 9 | 1.138 |
| +20 | +11 | 9 | 1.069 |
| +40 | +33 | 7 | 0.872 |
| +60 | +55 | 5 | 0.569 |
| +80 | +80 | 0 | 0.197 |

Table 1: Steady state error and torq exerted in the joint for a fixed set of positions using a 1138g load.

To correct these deviations from the ideal behavior, namely null steady state error and a low delay time in transient response, an external controller becomes necessary to improve these characteristics (Fig.6).
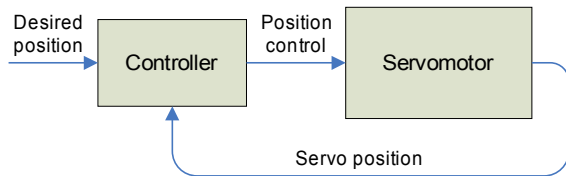


Fig. 6: Servo controller diagram.

## Adaptive Controller

As we can see, the servo behavior differs with the load angular position which makes it very hard to control having to considerer the beginning and final position to define a proper controller to adapt to each situation. Doing a theoretical analysis to our system we can understand where these complications are owing to. Let's considerer a weight of mass M connected to a joint through a link of length L.
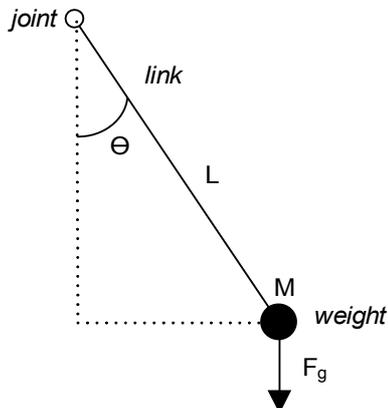


Fig. 7: System weight plus link connected to a movable joint.

The dynamics equation is given by:

$$\tau = \ddot{\theta} + \frac{c}{M \cdot L^2} \dot{\theta} + \frac{g}{L} \sin(\theta)$$

As can be seen, this system has a non linear dynamics owing to the $\sin(\theta)$ factor, making inappropriate the use of linear controllers. This is why the servo internal controller is inefficient to handle to all possible situations. In some circumstances, the factor $\sin(\theta)$ can be approximated to $\theta$, making suitable the use of linear controllers, nevertheless such approximation would limit $\theta$ variation to some degrees around an established reference angle, which is not the case.

As a result, as far as the mass approximates the maximum binary point (link and gravity force vector perpendicular) the response delay time and steady state error tend to increase deteriorating the controller's response. In the same way, these parameters are also related to the mass applied rising as far as we increase its weight.

### 3.3   Position Feedback Control Loop

- Blocks diagram

In order to minimize the steady state error and improve the transient response by the reduction of the delay time, an external controller was added with the desired position as input and the servo control position as output (Fig.6). Its model is described in Fig.8 and is based in a digital PID controller, whose derivation is represented by the difference module and the integrator by the delay module using the output control signal.
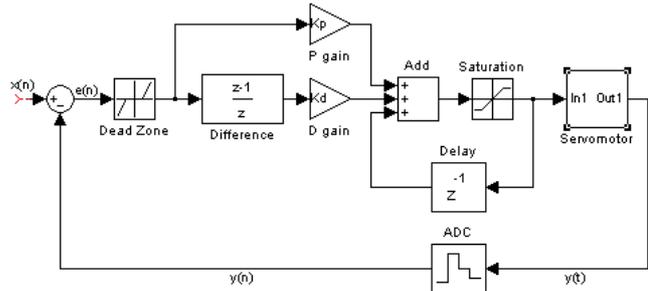


Fig. 8: External controller diagram blocks.

The desired position $x(n)$ and the measured position $y(n)$ (converted by the ADC) are compared and the result constitutes the error signal $e(n)$. To this signal is applied a proportional gain and a derivative compensation fundamental to improve the transient response. In addition, an integrative loop is used to clear the steady state error. The following differential equation describes the controller's functioning:

$$u(n) = u(n-1) + K_P \cdot e(n) + K_D \cdot [e(n) - e(n-1)]$$

4

Note that this equation represents a digital PID whose linear nature doesn't solve the non linearity problems. However it offers the possibility to adapt its behavior to each specific scenario by direct modification of its parameters, something not possible with the servo internal controller.

### 3.4 Adaptation to Load Variation

Several tests were made to prove the viability of this external controller in terms of improvement of response. Fig.9 compares open loop with closed loop response for a high load using only the proportional component.
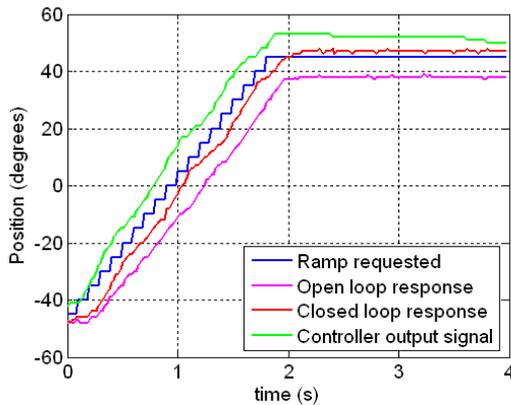


Fig. 9 – Open and closed loop ramp response for $K_P$=0.20 (924g load).

As can be observed the steady state error is eliminated and the delay time is reduced when applying a PI compensator. The green curve shows the controller output signal that enters in the servo mechanism with a higher position requisition than the desired in order to guarantee the effective position corresponds to the requested one.
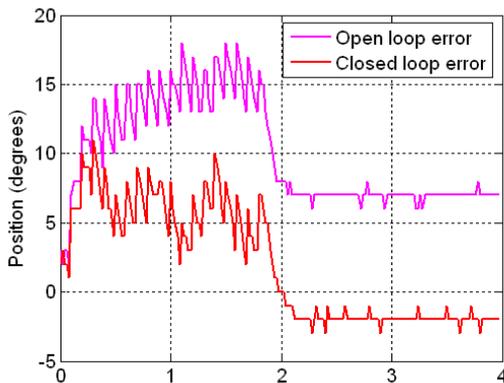


Fig. 10 – Open and closed loop error signal for $K_P$=0.20 (924g load).

Fig.10 shows the difference between the error signal in open and in closed loop confirming the proposed idea. The next figures introduce the derivative component as a reinforcement to improve even more the response quality. To demand a more exigent input we shrink the ramp step time update to the minimum – 20ms (PWM period) – with an amplitude update of 5 degrees. Defining a trajectory variation of 140 degrees (-90º to +50º) we will request the completion of the traject in only 1.12 seconds.
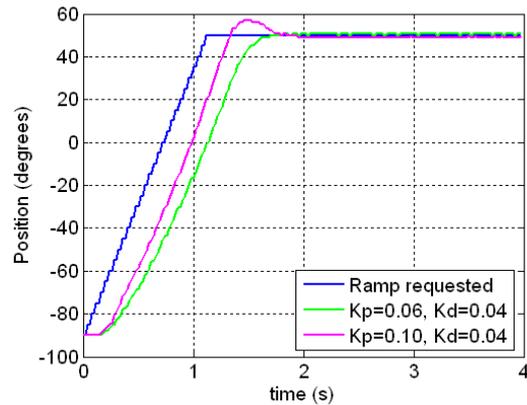


Fig. 11 – Closed loop ramp response for differnte $K_D$ parameters (924g load).
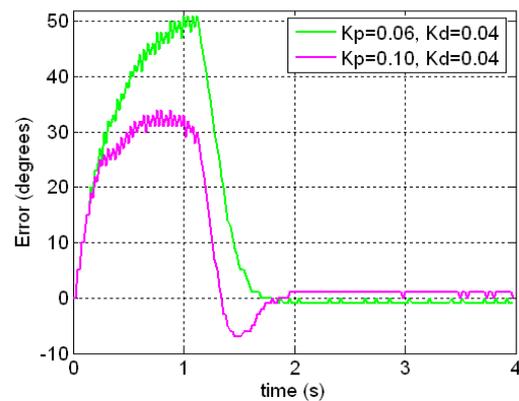


Fig. 12 – Closed loop error signal of Fig.11.

Sampling the response for different $K_P$ parameters maintaining fixed $K_D$ can be seen that $K_P$ affects the response delay time being so much closed to the requested trajectory as higher it is. Nevertheless it has to be limited to avoid instability which is reflected in overshoot and higher establishment times. Fig.11 and Fig.12 shows such situation when we increased $K_P$ from 0.06 to 0.10.

However, manipulating $K_D$ we can eliminate the overshoot and reduce the establishment time by its increase. Fig.13 confirms this idea: increasing the $K_D$ parameter the overshoot verified in Fig.12 were successfully controlled.

5
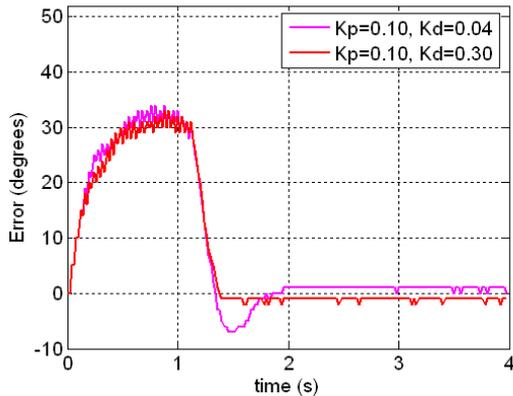
Fig. 13 – Closed loop error signal for an increased $K_P$ parameter.

In respect to the steady state error, the previous graphs proved its absence observing a maximum error of 3 degrees, derived to the "dead zone" block (Fig.8) necessary to prevent oscillation transmission to the controller blocks verified on the potentiometer reading.

## 3.5    Variable Velocity Control

An important subject in humanoid locomotion is trajectory planning, the ability to generate a trajectory from a collection of setpoints. Although we already were implementing trajectories using a ramp configuration (Fig.14) with a final position and mean velocity as setpoints, a huge disadvantage was present in this configuration: at the start and at the end of the trajectory a delta of Dirac is expected in the acceleration curve, something not possible on reality, which contributes to increase the servo response delay time and the overshoot.
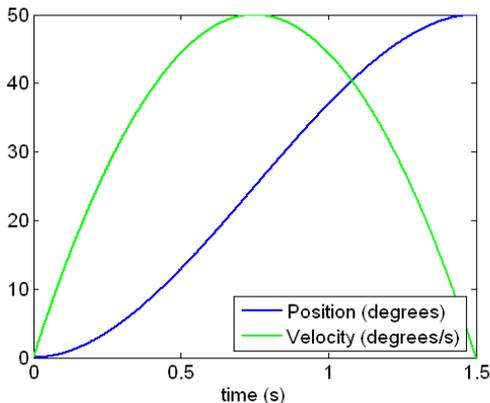


Fig. 14: Third order polynomial configuration trajectory.

To prevent this effect, instead of a pure ramp, we can generate a third polynomial configuration trajectory (Fig.15) which differentiates, by approximation, three stages: a first with a low acceleration, a second stage of greater acceleration and practically constant velocity, and a final one of deacceleration until the servo stops. In this configuration there is no deltas of Dirac in the acceleration curve and a soft locomotion is verified

during trajectory execution, with the extras of low response delay and establishment times (by overshoot diminution).

Fig. 15 shows the experimental results for the proposed strategy for a -70º to +70º trajectory to be fulfilled in 1.5 seconds with very encouraging results. It can be observed at the end of the traject that the soft stopping prevented an overshoot situation due the absence of a deacceleration peak.
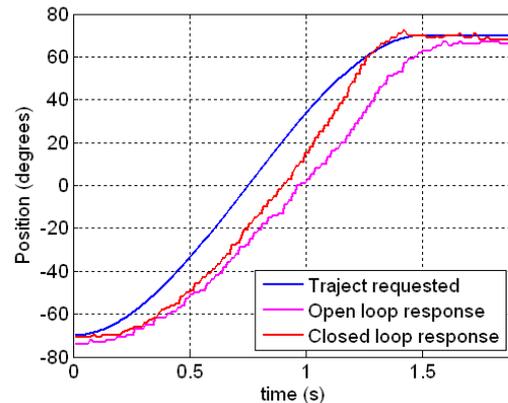


Fig. 15: Response for a $K_P$=0.15 and $K_D$=0.30, fulfilling a -70º to +70º trajectory in 1.5 seconds with a 1129g load.

On the other side, the steady state error continues to be eliminated as Fig.17 proves in a -90º to 0º trajectory to be completed in 1.0 seconds using a very heavy load. It can be observed that the ≈20º of steady state error in open loop is successfully cancelled when applying the external controller.
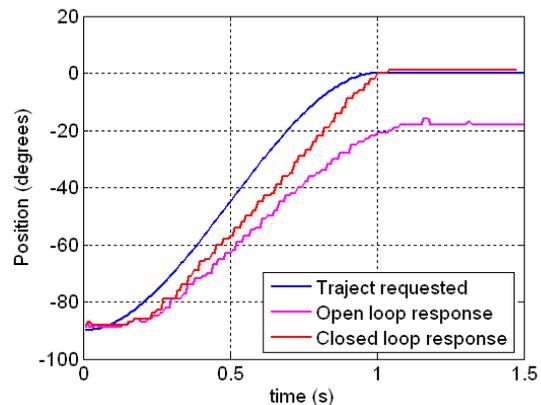


Fig. 16: Response for a $K_P$=0.20 and $K_D$=1.00 fulfilling a -90º to +90º trajectory in 1 second with a 1378g load.

6
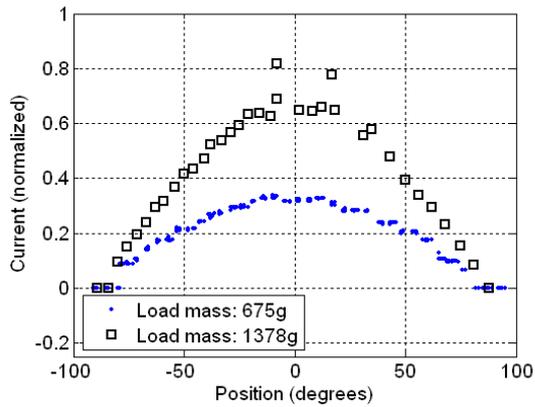
Fig. 17: Current consumption static measure (upwards direction).
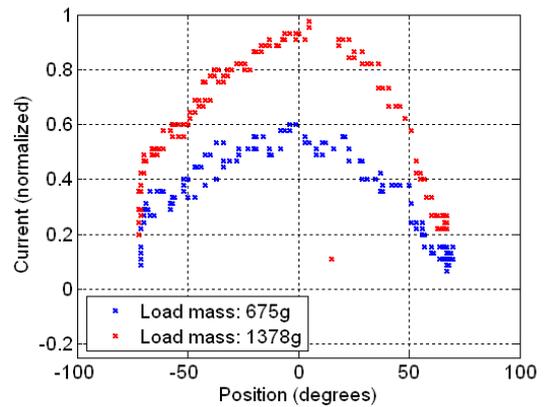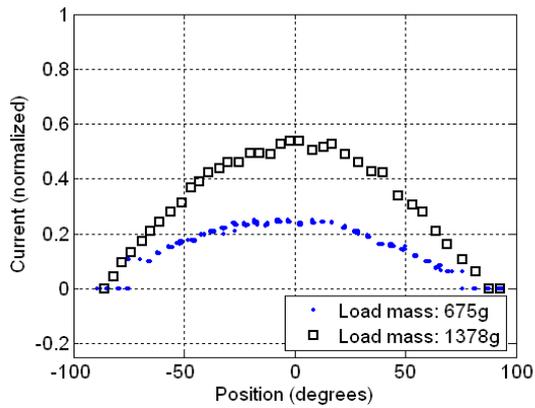

Fig. 18: Current consumption static measure (downwards direction).


Fig. 19: Current in open loop when performing a polynomial trajectory from -70º to +70º in 1.0 seconds.


Fig. 20: Current in open loop when performing a polynomial trajectory from -70º to +70º in 1.5 seconds.
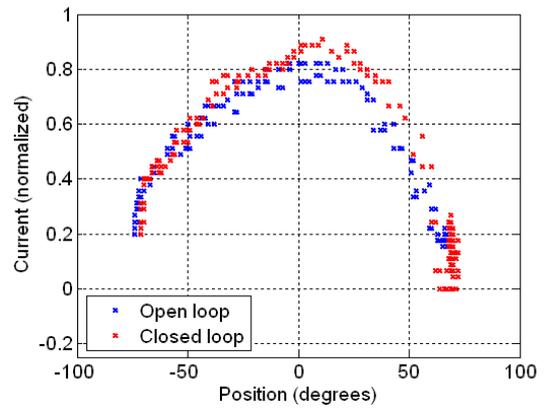

Fig. 21: Current consumption for the situation of Fig.15 (1129g load).
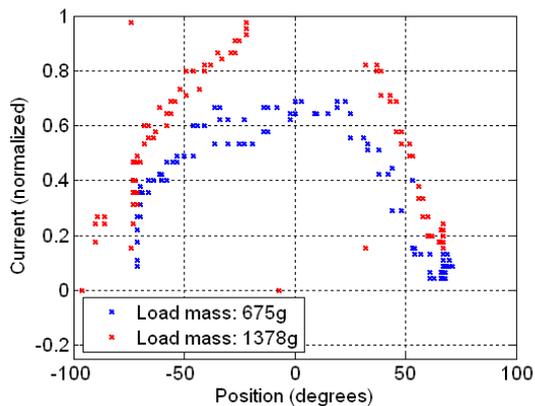
## 4. Conclusions

Referir a capcidade de controlo de velocidade a partir do controlo de posição.

Referir também o reenforço de estabilidade no controlo com a aplicação de trajectórias polinomias de 3ª ordem.